HHS Public Access

Author manuscript

Virology. Author manuscript; available in PMC 2018 February 01.

Published in final edited form as:

Virology. 2017 February ; 502: 63–72. doi:10.1016/j.virol.2016.12.017.

Recapitulation of treatment response patterns in a novel humanized mouse model for chronic hepatitis B virus infection

Benjamin Y. Winer[1], **Tiffany Huang**[1], **Benjamin E. Low**[2], **Cindy Avery**[2], **Mihai-Alexandru Pais**[1], **Gabriela Hrebikova**[1], **Evelyn Siu**[1], **Luis Chiriboga**[3], **Michael V. Wiles**[2], and **Alexander Ploss**[1,4]

[1]Department of Molecular Biology, Princeton University, 110 Lewis Thomas Laboratory, Washington Road, Princeton, New Jersey, NJ 08544, USA

[2]Department of Technology Evaluation and Development, The Jackson Laboratory 600 Main Street, Bar Harbor, Maine, 04609-1500 USA

[3]Department of Pathology, New York University Medical Center, New York, NY 10016, USA

Abstract

There are ~350 million chronic carriers of hepatitis B (HBV). While a prophylactic vaccine and drug regimens to suppress viremia are available, chronic HBV infection is rarely cured. HBV's limited host tropism leads to a scarcity of susceptible small animal models and is a hurdle to developing curative therapies. Mice that support engraftment with human hepatoctyes have traditionally been generated through crosses of murine liver injury models to immunodeficient backgrounds. Here, we describe the disruption of fumarylacetoacetate hydrolase directly in the NOD Rag1$^{-/-}$ IL2RγNULL (NRG) background using zinc finger nucleases. The resultant human liver chimeric mice sustain persistent HBV viremia for >90 days. When treated with standard of care therapy, HBV DNA levels decrease below detection but rebound when drug suppression is released, mimicking treatment response observed in patients. Our study highlights the utility of directed gene targeting approaches in zygotes to create new humanized mouse models for human diseases.

Keywords

Hepatitis B virus (HBV); humanized mice; antivirals; genome engineering

Introduction

Persistent infection with hepatitis B virus (HBV) is a global health problem afflicting approximately 400 million individuals worldwide, with Asia being disproportionally affected with over 130 million chronic cases (Tian and Jia, 2016). Chronic HBV carriers are

[4]To whom correspondence should be addressed: Alexander Ploss, aploss@princeton.edu, phone: (609) 258-7128, fax: (609) 258-1701.

at risk of developing fibrosis, cirrhosis or hepatocellular carcinoma (Trepo et al., 2014). HBV has a very limited host and cellular tropism, only robustly infecting human and chimpanzee hepatocytes. As a result of this limited tropism, and the subsequent paucity of animal models, HBV has been notoriously difficult to study. Furthermore, this has become more pressing due to the recent moratorium on using chimpanzees for research purposes due to ethical concerns.

Liver chimeric xenotransplantation mouse models have become a crucial experimental small animal model for the study of HBV as they can be robustly engrafted with primary human hepatocytes (PHHs), the natural host for HBV (Bissig et al., 2010; Dandri et al., 2001; Meuleman et al., 2005). The creation of liver chimeric mice requires that the xenorecipient is immune deficient to ensure that the tissue graft is not rejected. Furthermore, selective ablation of the endogenous murine hepatocytes is required to provide a proliferative signal and growth advantage for the transplanted human hepatocytes in the murine parenchyma (Billerbeck et al., 2013).

The best-characterized xenorecipient to date is a transgenic mouse that expresses the urokinase-type plasminogen activator (uPA) driven by the hepatocyte-specific albumin promoter (i.e. Alb-uPA mice). The overexpression of uPA in the murine liver leads to a hypofibrinogenemic state with accelerated hepatocyte death (Heckel et al., 1990). Alb-uPA mice have been crossed to different immunodeficient backgrounds, including severe combined immunodeficient (SCID), SCID/beige and recombinase-activating gene 2 ($Rag2^{-/-}$) interleukin 2 receptor gamma ($IL2\gamma^{NULL}$) deficient mice. Alb-uPA mice lacking mature B, T and/or NK cells can be engrafted with PHHs at a very high efficiency and have been shown to be susceptible to HBV, hepatitis C virus (HCV), hepatitis delta virus (HDV) and hepatitis E virus (HEV) infection (Allweiss et al., 2016; Dandri et al., 2001; Giersch et al., 2014; Mercer et al., 2001; Sayed et al., 2016). Unfortunately, Alb-uPA mice are relatively frail and hypofertile, so alternative liver injury models have been sought and created (reviewed in (Vercauteren et al., 2015)).

Expression of herpes simplex virus type-1 thymidine kinase (HSV tk) under the control of the mouse albumin promoter enables the selective killing of mouse hepatocytes by administration of the prodrug gancyclovir (Kosaka et al., 2013; Zhang et al., 2005). Human liver chimeric Alb-HSV tk transgenic mice on the NOD SCID $IL2\gamma^{NULL}$ (NOG) background have been shown to be susceptible to both HBV and HCV infection (Hasegawa et al., 2011). Alternatively, mice harboring a deficiency in fumarylacetoacetate hydrolase (FAH) have been bred to immunodeficient backgrounds (Azuma et al., 2007; Bissig et al., 2007; de Jong et al., 2014). FAH is the terminal enzyme in the tyrosine catabolic pathway; its absence leads to the buildup of toxic metabolites in murine hepatocytes leading to death. The administration of 2-(2-nitro-4-trifluoro-methylbenzoyl)-1,3-cyclohexanedione (NTBC, also known as nitisinone) inhibits the activity of an enzyme, 4-hydroxphenylpyruvate dioxygenase, upstream of FAH, thus abrogating the accumulation of the toxic metabolite fumarylacetoacetate to maintain $FAH^{-/-}$ mice in a healthy state (Al-Dhalimy et al., 2002). As a result, toxic injury can be induced at any time upon removal of NTBC and the growth advantage given to the engrafted human hepatocytes. This allows for transplantation to occur at the discretion of the researcher.

FAH$^{-/-}$ mice have been intercrossed with Rag2$^{-/-}$ IL2γ^{NULL} (FRG) (Azuma et al., 2007; Bissig et al., 2010; He et al., 2010) and completely backcrossed to the *NOD Rag1−/− IL2R*γ^{NULL} (FNRG) (de Jong et al., 2014) backgrounds. FRG and FNRG highly engrafted with human hepatocytes can sustain persistent HBV (Billerbeck et al., 2016; Bissig et al., 2010) and HCV infections (Bissig et al., 2010; de Jong et al., 2014). A considerable challenge in refining existing and developing new xenorecipient models is performing genetic modifications on previously characterized complex genetic backgrounds. Mutant alleles have been traditionally combined through inter- and backcrosses, a slow and expensive process. Genome engineering approaches using zinc finger nucleases (ZFNs), transcription activator-like (TAL) effector nucleases, and most recently, CRISPR/Cas9, have been pursued to create targeted, precise DNA breaks and consequently gene disruptions or modifications directly in zygotes (Kaneko and Mashimo, 2015). Proof-of-principle for these genome engineering methods for creating null alleles on the NSG and NRG backgrounds, which are most commonly used for creating humanized xenotransplantation models, was previously established by targeting exon 5 of the FAH gene (Li et al., 2014). Here, we used ZFNs to disrupt exon 9 of the murine FAH locus and compared them to FNRG mice which were previously generated through intercrosses of FAH$^{\Delta exon9}$ and NRG mice. We demonstrate that FNRG$^{\Delta exon9}$ mice reach a similar human hepatic chimerism as FNRG$^{\Delta exon5}$ mice following injection of PHHs. These human liver chimeric FNRG$^{\Delta exon9}$ mice can be persistently infected with HBV and exhibit similar treatment response profiles as observed in chronic HBV carriers treated with anti-HBV reverse transcriptase inhibitors.

Material and Methods

Generation of fumarylacetoacetate hydrolase (FAH) knockout on the complex NRG genetic background

A pair of zinc finger (ZFNs) nucleases targeting exon 9 of the FAH gene (5′ TACGTCCCACTTGGGCCAT and 5′ GGAAAAGCTTTGGAA) were purchased from Sigma Aldrich. ZFN encoding mRNAs were injected (2 ng/μl, cytoplasmic) into NRG zygotes, then transferred to pseudopregnant females. Founder animals were screened for modification to the locus by PCR and sequencing, those with detectable mutations were bred. Subsequent work used one line with a 172bp deletion in exon 9, designated (JAX ref) JR018454. This line is viable and fertile, and homozygous animals develop an obvious wasting phenotype in the absence of NTBC, consistent with the expected phenotype. Maintenance and breeding of homozygous mutant mice requires NTBC in the water at 16 mg/L. Additionally, use of a semisynthetic diet (SSNIFF: S9541-E006) was found to assist in maintaining the strain. This diet, produced by SSNIFF (Germany) is a modified Baker Diet that completely lacks Tyrosine and limits phenylalanine availability (0.6%). Routine genotyping uses PCR (primers F1: 5′-TCCACCAAGCATCACCATGTCTCA, R1: 5′TACACACTCCACTCACTGTTGCCA), Standard Taq (NEB: M0273), with a 70° C annealing temperature and 30 cycles. Resultant amplicons for wild-type and mutant alleles are 632 bp and 460 bp, respectively.

Assessment of liver injury due to FAH KO

To assess the level of liver injury due to the FAH KO, NTBC was removed for 9 days from 4-week-old mixed-sex (1F, 2M) mice (n=9; 3 WT, 3 HET, 3 HOM). Weight, ALT, and AST levels were monitored over the course of the 9 days. To assess liver damage, blood was drawn at three timepoints (initiation, day 7, termination). ALT and AST levels were assessed by the Clinical Assessment Service Core at the Jackson Laboratory, using a Beckman Coulter AU680 chemistry analyzer.

Generation of human liver chimeric mice

$FAH^{\Delta exon9}$ NRG and $FAH^{\Delta exon5}$ NRG mice were generated and transplanted as previously described (de Jong et al., 2014). Female mice of either strain greater than 6 weeks of age were transplanted with ca. 1×10^6 cryopreserved adult human hepatocytes. Primary hepatocytes were obtained from Bioreclamation (Westbury, NY). $FAH^{\Delta exon9}$ NRG mice were cycled on NTBC (Yecuris Inc., Tualatin, OR) supplemented in their water to block the build up of toxic metabolites and with water supplemented with L-phenylalanine (Sigma Aldrich, St. Luis MO) and 25 mM NaCl. $FAH^{\Delta exon9}$ NRG mice were maintained on the No-Tyr/Low-Phe diet (SSNIFF: S9541-E006).

Assessment of engraftment by human albumin ELISA

Levels of human albumin in mouse serum were quantified by ELISA; 96-well flat-bottomed plates (Nunc, Thermo Fischer Scientific, Witham MA) were coated with goat anti-human albumin antibody (1:500, Bethel) in coating buffer (1.59g Na_2CO_3, 2.93g $NaHCO_3$, 1L dH_2O, pH = 9.6) for 1 hour at 37°C. The plates were washed four times with wash buffer (0.05% Tween 20 (Sigma Aldrich, St. Luis MO) in 1x PBS) then incubated with superblock buffer (Fisher Scientific, Hampton NH) for 1 hour at 37°C. Plates were washed twice. Human serum albumin (Sigma Aldrich, St. Luis MO) was diluted to 1 μg/ml in sample diluent (10% Superblock, 90% wash buffer), then serial diluted 1:2 in 135 μl sample diluent to establish an albumin standard. Mouse serum (5 μl) was used for a 1:10 serial dilution in 135 μl sample diluent. The coated plates were incubated for 1 hour at 37°C, then washed three times. Mouse anti-human albumin (50 μl, 1:2000 in sample diluent, Abcam, Cambridge, UK) was added and plates were incubated for 2 hours at 37°C. Plates were washed four times and 50 μl of goat anti-mouse-HRP (1:10,000 in sample diluent, LifeTechnologies, Carlsbad, CA) was added and incubated for 1 hour at 37°C. Plates were washed six times. TMB (100 μl) substrate (Sigma Aldrich, St. Luis, MO) was added and the reaction was stopped with 12.5μl of 2N H_2SO_4. Absorbance was read at 450λ on the BertholdTech TriStar (Bad Wildbad, Germany).

Generation of hepatitis B virus stocks

HepG2.2.15 cells (Sells et al., 1987) were grown in media containing tetracycline until they reached a confluency of 100%. At this time media was changed to DMEM F12 media supplemented with 10% FBS, 1% Pen/Strep. Media from the HepG2.2.15 culture was collected every two to three days for approximately 3 weeks. The collected media was sterile filtered through a 0.22 μm filter (Millipore, Darmstadt Germany) and was then concentrated 100-fold using a stir cell concentrator (Millipore, Darmstadt Germany). After concentration,

the virus was run over a HiTrap heparin column (GE, Fairfield CA) to further concentrate and purify infectious virus particles from non-infectious sub-viral particles. Concentrated virus was applied to the heparin column, which was washed with 5 times column volume with wash buffer (20 mM phosphate buffer, 50 mM NaCl, pH= ~7). Afterwards, the virus was eluted with elution buffer (20 mM phosphate buffer, 2 M NaCl, pH= ~7). Once all virus was eluted, the viral stock was dialyzed using a dialysis cassette (Millipore, Darmstadt Germany). After dialysis, virus was aliquoted into cryovial tubes and cryopreserved at −80°C until use. The virus was passaged through a human liver chimeric mouse, resulting in high viremia. This mouse was euthanized and the serum diluted 1:20. A 200 μl aliquot of this 1:20 diluted virus was then used to infect all $FAH^{\Delta exon9}$ NRG mice. The same viral stock was used for all experiments.

HBV DNA isolation from mouse serum

HBV DNA was isolated following the Qiamp MinElute Virus Spin Kit (50), (Qiagen, Hilden, Germany). HBV DNA was eluted in 60 μl, and 5 μl was used per well in the HBV DNA qPCR reaction.

Total HBV DNA isolation from liver tissue

20–25 mg of liver tissue was weighed out from HBV infected $FAH^{\Delta exon9}$ NRG mice, which had been preserved in RNAlater (Thermo Fischer Scientific, Waltham MA) and stored at −80C. To isolate total HBV DNA from the liver sample, 100 μl of lysis buffer was added to the tissue (50 mM Tris-Base, 50 mM EDTA, 1% SDS, 100mM NaCl pH 8.0). The sample was further digested through the addition of 20 μl of Proteinase K per sample from a QIAMP DNA mini kit (Qiagen, Hilden, Germany) for 18 hours at 37°C. After digestion with Proteinase K, 1 μl of Rnase A (SigmaAldrich, St. Luis MO) was added to the lysate and incubated at room temperature for 2 minutes. We subsequently added 500 μl of AL lysis buffer (Qiagen, Hilden Germany) to the solution and incubated the sample at 70°C for 4 hours, vortexing the samples every 20 minutes to digest the tissue completely. Following this step, 500 μl of 100% EtOH were added and mixed thoroughly by inverting 10 times. This suspension was then applied to a Qiamp DNA mini kit column and centrifuged for 1 minute at 13,000 RPM to dry. The samples were spun again in new tubes for 1 min at 13,000 to dry. The DNA was then eluted with 50 μl of AE buffer and concentrations measured using a Nanodrop spectrophotometer (Thermo Fischer Scientific, Waltham MA).

Isolation of HBV cccDNA from total HBV DNA

A 25 μl aliquot of the respective total HBV DNA sample isolated from liver tissue was digested with 1 μl plasmid-safe DNAse (Epicentre, E3101K, Madison WI) to destroy all chromosomal DNA along with any linear form of HBV DNA. According to the manufacturers' instructions the reaction mix was incubated at 37°C for 30 minutes in order to digest the samples. Following the digestion, plasmid-safe DNase was heat inactivated by incubating the samples at 70°C for 30 minutes. The cccDNA was then purified using a DNA clean up and concentration kit (Zymo, Irvine, CA), eluted in 30 μl of sterile ddH_2O, and the residual amount of DNA quantified using a Nanodrop spectrophotomter. This resulted in a log drop in overall DNA concentration. Samples were either used immediately for HBV cccDNA quantification by qPCR or were stored at −20°C.

Total RNA isolation from liver tissue

20–25 mg of liver tissue was weighed out from HBV infected mice, which had been preserved in RNAlater and stored at −80C. We isolated total RNA using Qiagen RNAeasy kit (Qiagen, Hilden, Germany). Stainless steel beads (5 mm, Qiagen, Hilden Germany) and 350 μl RLT buffer were added to each sample tube RB (2ml, 990381, Qiagen, Hilden Germany). The liver tissue with RLT buffer and bead was then homogenized by the homogenizer (Fischer Scientific, Hampton NH). The sample was then eluted twice, first by the addition of 30 μl of RNase-free water to columns and centrifugation of the samples for 1 minute at 10,000 RPM, followed by another addition of 50 μl of RNase-free water.

Detection of HBV DNA by qPCR

A 5 μl aliquot of HBV DNA either isolated from mouse serum or from liver DNA was used per reaction well. We used the following primers and probes: CCGTCTGTGCCTTCTCATCTG (forward primer), AGTCCAAGAGTCCTCTTATGTAAGACCTT (reverse primer), and probe FAM-CCGTGTGCACTTCGCTTCACCTCTGC-TAMRA. Primers were kept at a concentration of 600 nM and probe at 300 nM final concentration in the reaction. A master mix was created containing 2X TaqMan reaction mix (AppliedBiosystems, Foster City, CA), primer/probe mix and ddH_2O. The master mix was then applied with the samples to the respective wells. We added 5 μl of the respective standards and the samples to the respective wells. The following PCR program was run on a Step One Plus qPCR machine (Life Technologies, Carlsbad CA): Denature 50°C for 5 min, 95°C for 10 min, followed by 40 cycles of 95°C for 15 sec, 56°C for 40 sec, and 72°C for 20 sec. Lastly, a melt curve was performed at 95°C for 10 sec, 65°C for 10 sec, 50°C for 5 sec, and 95°C for 5 sec.

Detection of HBV pre-genomic RNA by qPCR

A modified iTaq Universal SYBR Green One-Step qPCR kit (BioRad, Hercules, CA) protocol was used to quantify HBV pgRNA. A primer mix with each primer at 3 μM was created with the forward primer GAGTGTGGATTCGCACTCC and the reverse primer GAGGCGAGGGAGTTCTTCT. A master mix was created as follows per reaction: 5 μl of SYBR mix, 0.125 μl of RT, 1 μl of primer mix, and 1.875 μl of ddH_2O. The following cycling time was used: reverse transcription and amplification step at 50°C for 10 min and 95°C for 1 min; 40 cycles of 95°C 15 sec, and 60°C for 1 min. The melt curve was performed at 95°C for 5 sec, 65°C for 5 sec, 95°C for 15 sec, and 50°C for 5 sec.

Detection of HBV cccDNA by qPCR

A 5 μl aliquot of HBV DNA either isolated from mouse serum or from liver DNA was used per Rxn well. We used the following primers and probes: GTCTGTGCCTTCTCATCTGC (forward primer), AGTAACTCCACAGTAGCTCCAAATT (reverse primer), and probe FAM-TTCAAGCCTCCAAGCTGTGCCTTGGGTGGC-TAMRA. The final concentration of primers was 0.9 μM, 0.2 μM probe, and 4% DMSO. The following qPCR cycling was used: 95°C for 10 min, followed by 50 cycles of 95°C for 15 sec, and 61°C for 1 min. To confirm that cccDNA was detected and quantified specifically, primers were used that are biased for HBV cccDNA amplification over rcDNA which are

GCCTATTGATTGGAAAGTATGT (forward primer), AGCTGAGGCGGTATCTA (reverse primer) resulting in a 1,100 bp amplicon (Seeger and Sohn, 2014). Three DNA samples isolated from three separate $FAH^{\Delta exon9}$ NRG mice chronically infected with HBV were used. These samples had been treated with plasmid safe DNase as described in the HBV cccDNA isolation section of the material and methods (Figure 3H lanes 2–4). A negative control was utilized and showed no amplification (lane 5). The following PCR cycle was used in order to amplify the gene product 98°C 30 sec, followed by 36 cycles of 98°C for 10 seconds, 61°C for 30 seconds, 72°C for 45 seconds, followed by a final elongation step of 72°C for 2 minutes.

HBsAg ELISA measurements

Sera from mice were obtained through submandibular bleeding approximately every two weeks. Detection and quantification of HBsAg levels was performed by ELISA according to the manufacturer's instructions (GS HbsAg EIA 3.1, Bio-Rad, Hercules, CA). A 100 μl sample of a 1:20 serum dilution in 1x PBS was used in lieu of undiluted serum. Absorbance was read at 450λ on the BertholdTech TriStar (Bad Wildbad, Germany).

HbcAg immunohistology staining

Unconjugated polyclonal rabbit anti-Hepatitis B Virus Core Antigen antibody (Cell Marque Corp Cat# 216A-18 Lot# 17099, RRID: AB_1158068) raised against purified lysates of *Escherichia coli* clones containing the viral core DNA (Goodman et al., 1988; Sharma et al., 2002; Stahl et al., 1982). Antibody optimization was performed on formalin-fixed, paraffin-embedded murine HBV infected liver tissue based on known immunohistochemical conditions for HBV infected human liver samples utilizing the same antibody and run in parallel. We regarded hepatocytes clearly expressing cytoplasmic staining as positive for HBcAg. Chromogenic immunohistochemistry was performed on a Ventana Medical Systems Discovery XT instrument with online deparaffinization using Ventana's reagents and detection kits unless otherwise noted. Paraffin embedded tissues were sectioned at 4-μm. The marker was antigen retrieved in extended Cell Conditioner 1 (Tris EDTA, 52 minutes). Antibodies were applied neat with Hepatitis B Virus Core Antigen incubated for 2 hours. Primary antibody was detected with anti-rabbit horseradish peroxidase conjugated multimer, and incubated for 8 minutes. The complex was visualized with 3,3 diaminobenzidene and enhanced with copper sulfate. Slides were washed in distilled water, counterstained with hematoxylin, dehydrated and mounted with permanent media. Isotype negative controls, including wild type C57BL/6 non-infected murine liver tissue, were run in parallel with samples sets.

H&E staining

Paraffin embedded tissues were sectioned at 4 microns. H&E staining was performed using on a Leica ST5020 automated stainer. Paraffin was removed using xylene followed by graded ethyl alcohol dehydration. The sections were rehydrated with tap water and stained with Hematoxylin II for 2.0 minutes. After tap water wash, slides where clarified for 15 seconds, tap water washed and blued for 2.0 minutes. Sections were washed in tap and after an ethyl alcohol rinse, stained with Eosin-Y for 1.5 minutes. The sections were then

dehydrated in graded ethyl alcohol, cleared with xylene, and cover-slipped (all staining components were purchased from Thermo Scientific).

FAH staining

Immunohistochemistry was performed on formalin-fixed, paraffin-embedded human chimeric murine liver tissues using mouse anti-human (clone 2) FAH (Abcam). In brief, sections were deparaffinized in xylene (three changes), rehydrated through graded alcohols (three changes 100% ethanol, three changes 95% ethanol), and rinsed in distilled water. Antibody incubation and detection were carried out on a NEXes instrument (Ventana Medical Systems) using Ventana's reagent buffer and iVIEW detection kit unless otherwise noted. Endogenous peroxidase activity was blocked with hydrogen peroxide. Heat-induced epitope retrieval was performed in a 1200-W microwave oven at 100% power in 10 mM sodium citrate buffer (pH 6.0) for 20 min. Sections were allowed to cool for 30 min and then rinsed in distilled water. Mouse antihuman FAH was diluted 1:800 in Dulbecco's phosphate-buffered saline (PBS) (Invitrogen, Life Technologies) and incubated overnight at room temperature. Primary antibody was detected with biotinylated goat anti-mouse followed by application of streptavidin-HRP conjugate. The complex was visualized with 3,3-diaminobenzidine and enhanced with copper sulfate. Matched Ig isotype, at equivalent concentration and diluted in PBS, was used as a negative control. Upon completion of staining, all slides were washed in distilled water, counterstained with hematoxylin, dehydrated, and mounted with permanent medium. Stained slides were scanned at ×40 magnification using the Leica Microsystems SCN 400F Whole Slide Scanner. Images were viewed and captured using SlidePath's Digital Image Hub (Leica Microsystems).

Quantification of human hepatic chimerism by flowcytometry

To assess the engraftment levels of human hepatocytes in xenotransplanted animals, hepatocytes were isolated and fixed with 4% PFA in sterile 1X PBS for 20 minutes at RT. Cells were washed after the incubation period with wash Buffer (1X PBS, 1% FBS). Afterwards, the cells were permeabilized with permeabilization buffer (1X PBS, 0.1% Saponin, 1% FBS) for 20 minutes at RT. Cells were again washed after the incubation period with wash Buffer. Afterwards, hepatocytes were incubated with a PE-mouse anti-human CD81 (1:100 dilution) from BD pharmingen (Franklin Lakes, NJ) for 1 hour at 4°C. Cells were washed again to remove any unbound anti-human CD81 antibody. Stained cells had flow cytometry performed for detection of PE using an LSR II (BD, Franklin Lakes, NJ).

Quantification of the frequency of infected human hepatocytes

Images of ten randomly choses fields of views of HBcAg-stained liver sections were taken at a 10X magnification with an Evos FL cell system (Thermo Fischer Scientific, Waltham MA). The total number of cells in each image was counted along with the number of HbcAg positive cells. The total number of cells over the 10 images was 17,883 and the number of HbcAg positive cells was 338 resulting in 1.89% of the cells being infected with HBV. The hAlb level of ~1.5 mg/mL for the engrafted mouse means that ~5% of cells in the chimeric liver are human hepatocytes (Bissig et al., 2010). Based off these calculation approximately 37.8% of human hepatocytes were infected with HBV.

Results

Creation of FAH$^{\Delta exon9}$ knockout on the NOD Rag1−/− IL2Rγ^{NULL} background

A set of ZFNs designed to target murine FAH were purchased from Sigma Aldrich. The ZFN pairs were injected into multiple NRG oocytes. Mice were assayed for FAH deletion by PCR and sequencing with ultimately 17 distinct mutant lines identified. The descendants of mutant founder #1207 (JR018454) had the most promising mutation, a large deletion of 172 bp, easily detectable by PCR (Figure 1A) that resulted in a predicted premature STOP codon in exon 9.

Assessment of endogenous murine hepatocyte injury upon NTBC withdrawal

The FAH gene is primarily expressed in both the murine liver and kidneys. FAH mutants will develop liver and kidney injury if the protective drug NTBC is not supplied. To assess the endogenous murine hepatocyte injury in NRG FAH$^{\Delta exon9}$ [+/−] and [−/−] mice, NTBC was removed from their water for 9 days. Bleedings were performed at days 7 and 9 post-NTBC withdrawal, and ALT and AST levels were assessed in addition to the weight of the mice. Elevated ALT and AST levels, indicators of liver injury, were observed in FAH$^{-/-}$ mice following NTBC withdrawal, suggesting the presence of liver injury and thus an environment amenable to the engraftment of PHHs (Figure 1B and C). Both AST and ALT levels for Fah$^{+/-}$ and WT mice remained stable over the experimental time course.

To further confirm that NTBC withdrawal resulted in endogenous murine hepatocyte and kidney cell injury, both kidney and liver tissue from Fah$^{-/-}$ and WT mice were fixed in 4% PFA and paraffin embedded. H&E staining was performed on liver sections to assess any pathological changes. Severe diffuse tubular degeneration, increased basophilia, decreased brush border/blebbing, sloughed cells in tubular lumens, severe diffuse tubular dilation, and multifocal tubular dilatation were observed in the kidneys of FAH$^{\Delta exon9}$ *NRG* mice as compared to WT mice. Furthermore, several cysts were observed (Figure 2D–G).

In the livers of FAH$^{\Delta exon9}$ NRG mice, moderate diffuse hepatocellular hypertrophy was observed, and the cytoplasm was more basophilic than the WT or HET mice. Enlarged cells (cytomegaly) and enlarged nuclei (karyomegaly) were also observed (Figure 2H and I). While variation in cell and nuclear size as well as multinucleated hepatocytes are expected in rodent livers, all of these were more prominent in the Fah$^{-/-}$ livers than in the Fah$^{+/-}$ or WT mice (data not shown), indicating endogenous liver injury had occurred due to NTBC withdrawal and the subsequent build-up of hepatotoxic metabolites.

FAH$^{\Delta exon9}$ NOD Rag1−/− IL2Rγ^{NULL} mice can be robustly engrafted with human hepatocytes

Both FAH$^{\Delta exon9}$ and FAH$^{\Delta exon5}$ NRG mice (de Jong et al., 2014) were injected with PHHs and engraftment levels monitored by quantifying serum human albumin (hAlb) levels via ELISA. Three months after surgery, mice had high and stable levels of hAlb in their serum (1×10^2–10^4 μg/mL in serum), indicating stable engraftment (Figure 2A). The engraftment levels of FAH$^{\Delta exon9}$ NRG mice were overall about 10 fold lower than FAH$^{\Delta exon5}$ mice (Figure 2B). When the albumin concentration reached peak levels (ca. 10 weeks following

engraftment), liver sections were stained for human FAH (hFAH) to corroborate engraftment. Patches of hFAH positive cells were observed only in engrafted mice (Figure 2C right panel) and not in non-engrafted mice (Figure 2C left panel). To quantify more accurately the level of engraftment, single cell suspensions of hepatocytes isolated from a mouse with high serum hAlb (10^4 μg/mL) were stained with an anti-human CD81 antibody. Flow cytometric quantification demonstrated that approximately 21% of the hepatocytes were of human origin (Figure 2D). Taken together, these results demonstrate that FAH$^{\Delta exon9}$ NRG mice can be robustly engrafted with human hepatocytes.

Characterization of hepatitis B virus infection in human liver chimeric FAH$^{\Delta exon9}$ NRG mice

A stringent assessment of the functionality of engrafted human hepatocytes is their susceptibility to human hepatotropic viruses. HBV infects and replicates robustly only in differentiated, mature human hepatocytes. Thus, we next tested whether human liver chimeric FAH$^{\Delta exon9}$ NRG mice are susceptible to HBV infection. Humanized FAH$^{\Delta exon9}$ NRG mice were intravenously injected with tissue culture-derived HBV passaged through a human liver chimeric FAH$^{\Delta exon5}$ NRG mouse. Serum levels of HBV DNA (Figure 3A) and HBsAg (Figure 3B) were assessed by qPCR and HbsAg ELISA, respectively, in the chimeric animals at the indicated time-points. The time until establishment of HBV infection varied from 2–9 weeks post-HBV challenge, with more highly engrafted animals becoming viremic earlier, which is consistent with previous reports (Allweiss et al., 2014; Bissig et al., 2010; Dandri and Lutgehetmann, 2014). After 13 to 17 weeks following infection, mice were euthanized and their serum isolated and liver harvested. At the time of harvest, small sections from each lobe were preserved in RNAlater for analysis and quantification of total HBV DNA, HBV pre-genomic RNA (HBV pgRNA), and HBV covalently closed circular DNA (HBV cccDNA) by qPCR. Engrafted FAH$^{\Delta exon9}$ NRG mice became highly viremic as indicated by significant levels of total HBV DNA (1E2-1E6 GE/mL, Figure 3E), detectable levels of HBV cccDNA (1E3-1E4 Figure 3F and Figure 3H), and pgRNA (1E7-1E8 GE/mL, Figure 3G) in their livers. The range of HBV DNA correlates with the hAlb levels of the human engrafted mice, where higher levels of HBV DNA in the liver is observed mice with higher hAlb levels and therefore higher engraftment (Figure 3D). Furthermore, liver sections from HBV-challenged mice had more HbcAg stained hepatocytes as compared to unchallenged control mice (Figure 3C). It was determined that ~38% of the engrafted human hepatocytes were infected with HBV (see M&M for details about quantification).

Characterization of drug treatment with a HBV reverse transcriptase (RT) inhibitor in human liver chimeric FAH$^{\Delta exon9}$ NRG mice persistently infected with HBV

Finally, we aimed to test the utility of this chimeric mouse model to test antiviral therapies. While HBV is rarely cured, viremia can be suppressed with (combinations) of nucleot(s)ide inhibitors. To assess the effect of antiviral drugs on HBV infection in humanized FAH$^{\Delta exon9}$ NRG mice (n=4), mice persistently infected with HBV, as evidenced by high serum levels of HBV DNA for at least two time points (11 weeks post HBV challenge), were treated for 4 weeks with entecavir (ETV; 100 ng/g body weight of the animal), a nucleoside analog used to suppress HBV in chronic HBV patients. The treatment dose in mice was calculated based on the daily dose given to patients. Consistent with a previous report (Allweiss et al., 2014), levels of HBV DNA dropped 4–5 logs in all four mice (Figure 4A) after 4 weeks of

treatment, but HbsAg levels remained unchanged (**data not shown**). Two mice of the cohort died unrelated to the drug administration while the remaining two mice had ETV treatment suspended. Two weeks post-cessation of treatment, viral rebound was observed, with HBV DNA levels rising (Figure 4A) and ultimately plateauing at pre-treatment levels around 6 weeks thereafter. The levels of hAlb stayed stable during the course of ETV treatment and cessation of treatment (Figure 4B). Total HBV DNA was quantitated from liver tissue (Figure 4C) and was comparable to levels observed in the untreated cohort (Figure 3E). HBV cccDNA levels were unaffected by ETV treatment or ETV cessation (Figure 4D), and HBV cccDNA levels were comparable to untreated FAH$^{\Delta exon9}$ NRG mice. HBV pgRNA was also detected in the liver of ETV-treated FAH$^{\Delta exon9}$ NRG mice (Figure 4E), with HBV pgRNA levels being ~1.5 logs lower for ETV-treated mice as compared to untreated FAH$^{\Delta exon9}$ NRG mice.

Discussion

Humanized mice, in particular mice harboring a partially human liver, have become a crucial tool to study human liver (patho-)biology. Human liver chimeric mice have proven useful for pharmacokinetic and toxicologic studies (Nishimura et al., 2013; Xu et al., 2015a; Xu et al., 2014; Xu et al., 2015b), as highly engrafted animals exhibit human-like metabolic profiles (Tateno et al., 2004). Humanized mice have also proven to be an enabling technology to study human hepatotropic pathogens including human hepatitis viruses and the liver stages of parasites causing malaria in humans. Previous reports showed that human liver chimeric mice support persistent infections with HBV (Bissig et al., 2010; Dandri et al., 2001; Meuleman et al., 2005), HCV (Bissig et al., 2010; de Jong et al., 2014; Mercer et al., 2001; Meuleman et al., 2005), HDV (Lutgehetmann et al., 2012) and HEV (Allweiss et al., 2016; Sayed et al., 2016) and also faithfully recapitulate the hepatic stages of *Plasmodium (P.) falciparum* (Morosan et al., 2006; Sacci et al., 2006; VanBuskirk et al., 2009; Vaughan et al., 2012), *P. vivax* (Mikolajczak et al., 2015) and *P. ovale* (Dembele et al., 2014). A variety of liver injury models, including Alb-uPA (Dandri et al., 2001; Mercer et al., 2001; Meuleman et al., 2005), MUP-uPA (Carpentier et al., 2014; Heo et al., 2006), Alb-HSV-tk (Hasegawa et al., 2011) and FAH$^{-/-}$ mice (Azuma et al., 2007; Bissig et al., 2007; He et al., 2010), are being used to facilitate human hepatic engraftment on immunodeficient mouse backgrounds. Engraftment levels vary due to a number of factors, including the specific liver injury, the severity of the immunodeficiency and the quality (donor age, underlying liver diseases, fresh or cryopreserved) of the human hepatocytes (Kawahara et al., 2010; Vanwolleghem et al., 2010). FAH deficient mice are particularly attractive as they can be easily propagated, and the liver injury can be simply controlled by addition or removal of the liver protective drug NTBC.

The FAH gene has been independently inactivated several times. Chemical mutagenesis gave rise to mice harboring point mutations that led to frame shifts in exons 6 and 7 of the FAH gene (Aponte et al., 2001). The FAH gene has also been disrupted using traditional knock-out (FAH$^{\Delta exon5}$) (Grompe et al., 1993) and, more recently, using Crispr/Cas9-mediated approaches (Li et al., 2014), albeit the latter strain has not been extensively characterized. Here, we describe the disruption of FAH exon 9 on the NRG background using a nuclease directed by an allele-specific ZFN. FAH$^{\Delta exon9}$ NRG mice have a large deletion of 172 bp in

exon 9 while FAH$^{\Delta exon5}$ NRG mice (de Jong et al., 2014) have a 91 bp deletion in exon 5, each inactivating the FAH gene. The deletion in exon 9 of FAH$^{\Delta exon9}$ NRG leads to the same histopathology in both the liver and kidney that is observed in FAH$^{\Delta exon5}$ NRG mice, such as severe diffuse tubular degeneration, multifocal tubular dilatation, and cyst formation. While the histopathology is similar, FAH$^{\Delta exon9}$ NRG mice had human hepatocyte engraftment levels approximately 10 fold lower on average than FAH$^{\Delta exon5}$ NRG mice, as assessed by quantifying the concentration of serum hAlb. The lower engraftment levels of FAH$^{\Delta exon9}$ NRG mice might be explained by the varying severity of liver injury inflicted after NTBC withdrawal due to the slightly different genetic backgrounds of the two models. A possibility is that FAH$^{\Delta exon5}$ NRG mice have residual FAH activity. In both FAH$^{\Delta exon5}$ and FAH$^{\Delta exon9}$ NRG mice, there is a strong sex bias in the survival of animals upon engraftment, with male mice more susceptible to the buildup of toxic metabolites due to tyrosine catabolism upon NTBC withdrawal (data not shown). As a result, all FAH$^{\Delta exon9}$ NRG mice used in this study were female mice, and liver injury had to be very finely controlled. In contrast to FAH$^{\Delta exon5}$ NRG, FAH$^{\Delta exon9}$ NRG mice were kept on a diet low in aromatic amino acids to prevent premature death; upon NTBC withdrawal, the mortality rate was high. The high mortality rate of FAH$^{\Delta exon9}$ NRG mice on regular chow is likely due to aromatic amino acids being present, leading to the buildup of toxic metabolites in these mice. It is also noteworthy that in engraftment experiments, FAH$^{\Delta exon9}$ NRG mice were kept on water supplemented with L-phenylalanine once NTBC was removed to help control induction of endogenous murine liver damage. Phenylalanine is converted to tyrosine by phenyalanine hydrolase, facilitating the build-up of toxic metabolites upon withdrawal of NTBC. The combination of a diet low in aromatic amino acids and water supplemented with phenylalanine suggests that fine tuning is required to reach optimum levels of aromatic amino acids in FAH$^{\Delta exon9}$ NRG mice for facilitating endogenous liver damage in murine hepatocytes and the robust engraftment of human hepatocytes. Further optimization of the phenyl water/NTBC cycling, as well as the engraftment procedure, should further improve the human hepatocyte engraftment. This combination of phenyl water/NTBC cycling presumably provides greater control of induction of liver injury in this model versus the current FAH$^{\Delta exon5}$ NRG mice.

We have shown here that FAH$^{\Delta exon9}$ NRG mice, similar to immunodeficient FAH$^{\Delta exon5}$ mice, are susceptible to HBV infection once engrafted with human hepatocytes (Billerbeck et al., 2016; Bissig et al., 2010). All viral intermediates can be observed in these mice, including HbsAg in serum, HBcAg-positive human hepatocytes, HBV total DNA in serum and liver, HBV pgRNA and HBV cccDNA.

The standard of care treatment for HBV is pegylated interferon and/or nucleos(t)ide analogs. Nucleos(t)ide analogs suppress HBV viremia by targeting the viral polymerase. ETV and tenofovir (TDF) have the highest barrier to resistance (Lazarevic, 2014). As a result, we decided to treat with ETV a cohort of FAH$^{\Delta exon9}$ NRG mice chronically infected with HBV. Upon treatment with ETV (100 ng/g weight mouse), HBV DNA levels significantly decreased in the serum by ~4–5 logs, which is approximately one log more than what has been observed in human hepatocyte-engrafted uPA-SCID mice (Allweiss et al., 2014). This approximately one log greater reduction of HBV DNA in serum could be due to the fact that FAH$^{\Delta exon9}$ NRG mice had on average approximately one log lower engraftment levels,

making the ETV dosage per human hepatocyte greater than in the uPA-SCID mice (Allweiss et al., 2014). However, this would only be the case if ETV is metabolized at a faster rate by human hepatocytes as compared to murine hepatocytes. Upon withdrawal of ETV, HBV DNA levels in the serum of FAH$^{\Delta exon9}$ NRG rebounded. This is the first time that viral rebound has been shown in a human liver chimeric mouse model upon cessation of ETV treatment. This is similar to what is observed in chronic HBV patients that have developed resistance to ETV treatment (Tenney et al., 2004). Resistance to ETV is rather rare, with rates at <1.2% unless a patient has been previously treated with lamivudine (LAM) and developed LAM escape mutations (Chang et al., 2010). These LAM-resistant strains of HBV become resistant to ETV 51% of the time, with the M204V strain comprising the majority of ETV-resistant viruses (Lee et al., 2013; Tenney et al., 2009). Upon viral breakthrough in these patients, HBV DNA levels rebound with a corresponding increase in ALT and AST levels and liver damage.

We have shown here that FAH$^{\Delta exon9}$ NRG mice have a non-functional FAH gene which leads to endogenous damage of murine cells in both the liver and kidney, providing a growth advantage for engrafted human hepatocytes. Once engrafted, these mice are capable of being infected with HBV and upon treatment with ETV, show a reduction in HBV DNA levels in their serum. Cessation of ETV treatment leads to HBV DNA levels rebounding, which is in accordance with observations in chronic HBV patients who have been treated with nucleoside analogs and subsequently developed viral escape mutations or were non-compliant in their treatment. These data in aggregate show the utility of this model for investigating HBV pathology.

Recently, a few studies have engrafted mice with both human hepatocytes and hematopoietic stem cells, creating mice with both a human/mouse chimeric liver and a partial human immune system. These mouse models have been utilized to investigate HBV or HCV pathogenesis and the host immune response to infection (Bility et al., 2014; Billerbeck et al., 2016; Strick-Marchand et al., 2015; Washburn et al., 2011). The NOD Rag1−/− IL2Rγ^{NULL} background is amenable to human hematopoietic stem cell engraftment (Brehm et al., 2010; Pearson et al., 2008). Thus, FAH$^{\Delta exon9}$ NRG mice can be dually engrafted with both human hepatocytes and hematopoietic stem cells, allowing for the investigation of host immune responses in the context of HBV infection. In total, the FAH$^{\Delta exon9}$ NRG mouse model generated here is a versatile xenorecipient model for the investigation of HBV pathogenesis.

Acknowledgments

HepG2.2.15 cells were kindly provided by Christoph Seeger (Fox Chase Cancer Center). We would like to thank Rosalinda Doty for her skillful pathology work and Jenna Gaska for her helpful discussions and edits of this manuscript. We would also like to thank Gabriel Lipkowitz for his assistance with experiments. This study is supported by grants from the National Institutes of Health (R01 AI079031, R01 AI107301, R21AI117213 to AP), a Research Scholar Award from the American Cancer Society (RSG-15-048-01-MPC to AP), a Burroughs Wellcome Fund Award for Investigators in Pathogenesis (to AP) and a Graduate fellowship from the Health Grand Challenge from the Global Health Fund of Princeton University (to BYW). The NYU Experimental Pathology Immunohistochemistry Core Laboratory is supported in part by the Laura and Isaac Perlmutter Cancer Center Support Grant; NIH/NCI P30CA016087″ and the National Institutes of Health S10 Grants; NIH/ORIP S10OD01058 and S10OD018338. BYW is a recipient of F31 NIH/NRSA Ruth L. Kirschstein Predoctoral awarded from the NIAID, MVW, CA and BEL were funded by The Jackson Laboratory. MAP was supported by a fellowship from Evangelisches Studienwerk Villigst.

References

Al-Dhalimy M, Overturf K, Finegold M, Grompe M. Long-term therapy with NTBC and tyrosine-restricted diet in a murine model of hereditary tyrosinemia type I. Molecular genetics and metabolism. 2002; 75:38–45. [PubMed: 11825062]

Allweiss L, Gass S, Giersch K, Groth A, Kah J, Volz T, Rapp G, Schobel A, Lohse AW, Polywka S, Pischke S, Herker E, Dandri M, Lutgehetmann M. Human liver chimeric mice as a new model of chronic hepatitis E virus infection and preclinical drug evaluation. J Hepatol. 2016; 64:1033–1040. [PubMed: 26805671]

Allweiss L, Volz T, Lutgehetmann M, Giersch K, Bornscheuer T, Lohse AW, Petersen J, Ma H, Klumpp K, Fletcher SP, Dandri M. Immune cell responses are not required to induce substantial hepatitis B virus antigen decline during pegylated interferon-alpha administration. Journal of hepatology. 2014; 60:500–507. [PubMed: 24398036]

Aponte JL, Sega GA, Hauser LJ, Dhar MS, Withrow CM, Carpenter DA, Rinchik EM, Culiat CT, Johnson DK. Point mutations in the murine fumarylacetoacetate hydrolase gene: Animal models for the human genetic disorder hereditary tyrosinemia type 1. Proc Natl Acad Sci U S A. 2001; 98:641–645. [PubMed: 11209059]

Azuma H, Paulk N, Ranade A, Dorrell C, Al-Dhalimy M, Ellis E, Strom S, Kay MA, Finegold M, Grompe M. Robust expansion of human hepatocytes in Fah−/−/Rag2−/−/Il2rg−/− mice. Nat Biotechnol. 2007; 25:903–910. [PubMed: 17664939]

Bility MT, Cheng L, Zhang Z, Luan Y, Li F, Chi L, Zhang L, Tu Z, Gao Y, Fu Y, Niu J, Wang F, Su L. Hepatitis B virus infection and immunopathogenesis in a humanized mouse model: induction of human-specific liver fibrosis and M2-like macrophages. PLoS Pathog. 2014; 10:e1004032. [PubMed: 24651854]

Billerbeck E, de Jong Y, Dorner M, de la Fuente C, Ploss A. Animal models for hepatitis C. Curr Top Microbiol Immunol. 2013; 369:49–86. [PubMed: 23463197]

Billerbeck E, Mommersteeg MC, Shlomai A, Xiao JW, Andrus L, Bhatta A, Vercauteren K, Michailidis E, Dorner M, Krishnan A, Charlton MR, Chiriboga L, Rice CM, de Jong YP. Humanized mice efficiently engrafted with fetal hepatoblasts and syngeneic immune cells develop human monocytes and NK cells. J Hepatol. 2016; 65:334–343. [PubMed: 27151182]

Bissig KD, Le TT, Woods NB, Verma IM. Repopulation of adult and neonatal mice with human hepatocytes: a chimeric animal model. Proceedings of the National Academy of Sciences of the United States of America. 2007; 104:20507–20511. [PubMed: 18077355]

Bissig KD, Wieland SF, Tran P, Isogawa M, Le TT, Chisari FV, Verma IM. Human liver chimeric mice provide a model for hepatitis B and C virus infection and treatment. J Clin Invest. 2010; 120:924–930. [PubMed: 20179355]

Brehm MA, Cuthbert A, Yang C, Miller DM, DiIorio P, Laning J, Burzenski L, Gott B, Foreman O, Kavirayani A, Herlihy M, Rossini AA, Shultz LD, Greiner DL. Parameters for establishing humanized mouse models to study human immunity: analysis of human hematopoietic stem cell engraftment in three immunodeficient strains of mice bearing the IL2rgamma(null) mutation. Clin Immunol. 2010; 135:84–98. [PubMed: 20096637]

Carpentier A, Tesfaye A, Chu V, Nimgaonkar I, Zhang F, Lee SB, Thorgeirsson SS, Feinstone SM, Liang TJ. Engrafted human stem cell-derived hepatocytes establish an infectious HCV murine model. J Clin Invest. 2014; 124:4953–4964. [PubMed: 25295540]

Chang TT, Lai CL, Kew Yoon S, Lee SS, Coelho HS, Carrilho FJ, Poordad F, Halota W, Horsmans Y, Tsai N, Zhang H, Tenney DJ, Tamez R, Iloeje U. Entecavir treatment for up to 5 years in patients with hepatitis B e antigen-positive chronic hepatitis B. Hepatology. 2010; 51:422–430. [PubMed: 20049753]

Dandri M, Burda MR, Torok E, Pollok JM, Iwanska A, Sommer G, Rogiers X, Rogler CE, Gupta S, Will H, Greten H, Petersen J. Repopulation of mouse liver with human hepatocytes and in vivo infection with hepatitis B virus. Hepatology. 2001; 33:981–988. [PubMed: 11283864]

Dandri M, Lutgehetmann M. Mouse models of hepatitis B and delta virus infection. J Immunol Methods. 2014; 410:39–49. [PubMed: 24631647]

de Jong YP, Dorner M, Mommersteeg MC, Xiao JW, Balazs AB, Robbins JB, Winer BY, Gerges S, Vega K, Labitt RN, Donovan BM, Giang E, Krishnan A, Chiriboga L, Charlton MR, Burton DR, Baltimore D, Law M, Rice CM, Ploss A. Broadly neutralizing antibodies abrogate established hepatitis C virus infection. Sci Transl Med. 2014; 6:254ra129.

Dembele L, Franetich JF, Lorthiois A, Gego A, Zeeman AM, Kocken CH, Le Grand R, Dereuddre-Bosquet N, van Gemert GJ, Sauerwein R, Vaillant JC, Hannoun L, Fuchter MJ, Diagana TT, Malmquist NA, Scherf A, Snounou G, Mazier D. Persistence and activation of malaria hypnozoites in long-term primary hepatocyte cultures. Nat Med. 2014; 20:307–312. [PubMed: 24509527]

Giersch K, Helbig M, Volz T, Allweiss L, Mancke LV, Lohse AW, Polywka S, Pollok JM, Petersen J, Taylor J, Dandri M, Lutgehetmann M. Persistent hepatitis D virus mono-infection in humanized mice is efficiently converted by hepatitis B virus to a productive co-infection. Journal of hepatology. 2014; 60:538–544. [PubMed: 24280293]

Goodman ZD, Langloss JM, Bratthauer GL, Ishak K. Immunohistochemical localization of hepatitis B surface antigen and hepatitis B core antigen in tissue sections. A source of false positive staining. Am J Clin Pathol. 1988; 89:533–537. [PubMed: 3281436]

Grompe M, al-Dhalimy M, Finegold M, Ou CN, Burlingame T, Kennaway NG, Soriano P. Loss of fumarylacetoacetate hydrolase is responsible for the neonatal hepatic dysfunction phenotype of lethal albino mice. Genes Dev. 1993; 7:2298–2307. [PubMed: 8253378]

Hasegawa M, Kawai K, Mitsui T, Taniguchi K, Monnai M, Wakui M, Ito M, Suematsu M, Peltz G, Nakamura M, Suemizu H. The reconstituted ‘humanized liver’ in TK-NOG mice is mature and functional. Biochem Biophys Res Commun. 2011; 405:405–410. [PubMed: 21238430]

He Z, Zhang H, Zhang X, Xie D, Chen Y, Wangensteen KJ, Ekker SC, Firpo M, Liu C, Xiang D, Zi X, Hui L, Yang G, Ding X, Hu Y, Wang X. Liver xeno-repopulation with human hepatocytes in Fah−/−Rag2−/− mice after pharmacological immunosuppression. Am J Pathol. 2010; 177:1311–1319. [PubMed: 20651238]

Heckel JL, Sandgren EP, Degen JL, Palmiter RD, Brinster RL. Neonatal bleeding in transgenic mice expressing urokinase-type plasminogen activator. Cell. 1990; 62:447–456. [PubMed: 1696178]

Heo J, Factor VM, Uren T, Takahama Y, Lee JS, Major M, Feinstone SM, Thorgeirsson SS. Hepatic precursors derived from murine embryonic stem cells contribute to regeneration of injured liver. Hepatology. 2006; 44:1478–1486. [PubMed: 17133486]

Kaneko T, Mashimo T. Creating knockout and knockin rodents using engineered endonucleases via direct embryo injection. Methods Mol Biol. 2015; 1239:307–315. [PubMed: 25408415]

Kawahara T, Toso C, Douglas DN, Nourbakhsh M, Lewis JT, Tyrrell DL, Lund GA, Churchill TA, Kneteman NM. Factors affecting hepatocyte isolation, engraftment, and replication in an in vivo model. Liver Transpl. 2010; 16:974–982. [PubMed: 20677288]

Kosaka K, Hiraga N, Imamura M, Yoshimi S, Murakami E, Nakahara T, Honda Y, Ono A, Kawaoka T, Tsuge M, Abe H, Hayes CN, Miki D, Aikata H, Ochi H, Ishida Y, Tateno C, Yoshizato K, Sasaki T, Chayama K. A novel TK-NOG based humanized mouse model for the study of HBV and HCV infections. Biochem Biophys Res Commun. 2013

Lazarevic I. Clinical implications of hepatitis B virus mutations: recent advances. World J Gastroenterol. 2014; 20:7653–7664. [PubMed: 24976703]

Lee GH, Aung MO, Dan YY, Lee YM, Mak B, Low HC, Lim K, Thwin MA, Tan PS, Lim SG. Do different lamivudine-resistant hepatitis B genotypes carry the same risk of entecavir resistance? J Med Virol. 2013; 85:26–33. [PubMed: 23023992]

Li F, Cowley DO, Banner D, Holle E, Zhang L, Su L. Efficient genetic manipulation of the NOD-Rag1−/−IL2RgammaC-null mouse by combining in vitro fertilization and CRISPR/Cas9 technology. Scientific reports. 2014; 4:5290. [PubMed: 24936832]

Lutgehetmann M, Mancke LV, Volz T, Helbig M, Allweiss L, Bornscheuer T, Pollok JM, Lohse AW, Petersen J, Urban S, Dandri M. Humanized chimeric uPA mouse model for the study of hepatitis B and D virus interactions and preclinical drug evaluation. Hepatology. 2012; 55:685–694. [PubMed: 22031488]

Mercer DF, Schiller DE, Elliott JF, Douglas DN, Hao C, Rinfret A, Addison WR, Fischer KP, Churchill TA, Lakey JR, Tyrrell DL, Kneteman NM. Hepatitis C virus replication in mice with chimeric human livers. Nature medicine. 2001; 7:927–933.

Meuleman P, Libbrecht L, De Vos R, de Hemptinne B, Gevaert K, Vandekerckhove J, Roskams T, Leroux-Roels G. Morphological and biochemical characterization of a human liver in a uPA-SCID mouse chimera. Hepatology. 2005; 41:847–856. [PubMed: 15791625]

Mikolajczak SA, Vaughan AM, Kangwanrangsan N, Roobsoong W, Fishbaugher M, Yimamnuaychok N, Rezakhani N, Lakshmanan V, Singh N, Kaushansky A, Camargo N, Baldwin M, Lindner SE, Adams JH, Sattabongkot J, Kappe SH. Plasmodium vivax Liver Stage Development and Hypnozoite Persistence in Human Liver-Chimeric Mice. Cell Host Microbe. 2015; 17:526–535. [PubMed: 25800544]

Morosan S, Hez-Deroubaix S, Lunel F, Renia L, Giannini C, Van Rooijen N, Battaglia S, Blanc C, Eling W, Sauerwein R, Hannoun L, Belghiti J, Brechot C, Kremsdorf D, Druilhe P. Liver-stage development of Plasmodium falciparum, in a humanized mouse model. The Journal of infectious diseases. 2006; 193:996–1004. [PubMed: 16518762]

Nishimura T, Hu Y, Wu M, Pham E, Suemizu H, Elazar M, Liu M, Idilman R, Yurdaydin C, Angus P, Stedman C, Murphy B, Glenn J, Nakamura M, Nomura T, Chen Y, Zheng M, Fitch WL, Peltz G. Using chimeric mice with humanized livers to predict human drug metabolism and a drug-drug interaction. The Journal of pharmacology and experimental therapeutics. 2013; 344:388–396. [PubMed: 23143674]

Pearson T, Shultz LD, Miller D, King M, Laning J, Fodor W, Cuthbert A, Burzenski L, Gott B, Lyons B, Foreman O, Rossini AA, Greiner DL. Non-obese diabetic-recombination activating gene-1 (NOD-Rag1 null) interleukin (IL)-2 receptor common gamma chain (IL2r gamma null) null mice: a radioresistant model for human lymphohaematopoietic engraftment. Clin Exp Immunol. 2008; 154:270–284. [PubMed: 18785974]

Sacci JB Jr, Alam U, Douglas D, Lewis J, Tyrrell DL, Azad AF, Kneteman NM. Plasmodium falciparum infection and exoerythrocytic development in mice with chimeric human livers. Int J Parasitol. 2006; 36:353–360. [PubMed: 16442544]

Sayed IM, Verhoye L, Cocquerel L, Abravanel F, Foquet L, Montpellier C, Debing Y, Farhoudi A, Wychowski C, Dubuisson J, Leroux-Roels G, Neyts J, Izopet J, Michiels T, Meuleman P. Study of hepatitis E virus infection of genotype 1 and 3 in mice with humanised liver. Gut. 2016

Seeger C, Sohn JA. Targeting Hepatitis B Virus With CRISPR/Cas9. Molecular therapy. Nucleic acids. 2014; 3:e216. [PubMed: 25514649]

Sells MA, Chen ML, Acs G. Production of hepatitis B virus particles in Hep G2 cells transfected with cloned hepatitis B virus DNA. Proceedings of the National Academy of Sciences of the United States of America. 1987; 84:1005–1009. [PubMed: 3029758]

Sharma RR, Dhiman RK, Chawla Y, Vasistha RK. Immunohistochemistry for core and surface antigens in chronic hepatitis. Tropical gastroenterology: official journal of the Digestive Diseases Foundation. 2002; 23:16–19. [PubMed: 12170914]

Stahl S, MacKay P, Magazin M, Bruce SA, Murray K. Hepatitis B virus core antigen: synthesis in Escherichia coli and application in diagnosis. Proceedings of the National Academy of Sciences of the United States of America. 1982; 79:1606–1610. [PubMed: 7041126]

Strick-Marchand H, Dusseaux M, Darche S, Huntington ND, Legrand N, Masse-Ranson G, Corcuff E, Ahodantin J, Weijer K, Spits H, Kremsdorf D, Di Santo JP. A novel mouse model for stable engraftment of a human immune system and human hepatocytes. PLoS One. 2015; 10:e0119820. [PubMed: 25782010]

Tateno C, Yoshizane Y, Saito N, Kataoka M, Utoh R, Yamasaki C, Tachibana A, Soeno Y, Asahina K, Hino H, Asahara T, Yokoi T, Furukawa T, Yoshizato K. Near completely humanized liver in mice shows human-type metabolic responses to drugs. Am J Pathol. 2004; 165:901–912. [PubMed: 15331414]

Tenney DJ, Levine SM, Rose RE, Walsh AW, Weinheimer SP, Discotto L, Plym M, Pokornowski K, Yu CF, Angus P, Ayres A, Bartholomeusz A, Sievert W, Thompson G, Warner N, Locarnini S, Colonno RJ. Clinical emergence of entecavir-resistant hepatitis B virus requires additional substitutions in virus already resistant to Lamivudine. Antimicrobial agents and chemotherapy. 2004; 48:3498–3507. [PubMed: 15328117]

Tenney DJ, Rose RE, Baldick CJ, Pokornowski KA, Eggers BJ, Fang J, Wichroski MJ, Xu D, Yang J, Wilber RB, Colonno RJ. Long-term monitoring shows hepatitis B virus resistance to entecavir in

nucleoside-naive patients is rare through 5 years of therapy. Hepatology. 2009; 49:1503–1514. [PubMed: 19280622]

Tian Q, Jia J. Hepatitis B virus genotypes: epidemiological and clinical relevance in Asia. Hepatology international. 2016

Trepo C, Chan HL, Lok A. Hepatitis B virus infection. Lancet. 2014; 384:2053–2063. [PubMed: 24954675]

VanBuskirk KM, O'Neill MT, De La Vega P, Maier AG, Krzych U, Williams J, Dowler MG, Sacci JB Jr, Kangwanrangsan N, Tsuboi T, Kneteman NM, Heppner DG Jr, Murdock BA, Mikolajczak SA, Aly AS, Cowman AF, Kappe SH. Preerythrocytic, live-attenuated Plasmodium falciparum vaccine candidates by design. Proceedings of the National Academy of Sciences of the United States of America. 2009; 106:13004–13009. [PubMed: 19625622]

Vanwolleghem T, Libbrecht L, Hansen BE, Desombere I, Roskams T, Meuleman P, Leroux-Roels G. Factors determining successful engraftment of hepatocytes and susceptibility to hepatitis B and C virus infection in uPA-SCID mice. Journal of hepatology. 2010; 53:468–476. [PubMed: 20591528]

Vaughan AM, Mikolajczak SA, Wilson EM, Grompe M, Kaushansky A, Camargo N, Bial J, Ploss A, Kappe SH. Complete Plasmodium falciparum liver-stage development in liver-chimeric mice. J Clin Invest. 2012; 122:3618–3628. [PubMed: 22996664]

Vercauteren K, de Jong YP, Meuleman P. Animal models for the study of HCV. Current opinion in virology. 2015; 13:67–74. [PubMed: 26304554]

Washburn ML, Bility MT, Zhang L, Kovalev GI, Buntzman A, Frelinger JA, Barry W, Ploss A, Rice CM, Su L. A humanized mouse model to study hepatitis C virus infection, immune response, and liver disease. Gastroenterology. 2011; 140:1334–1344. [PubMed: 21237170]

Xu D, Michie SA, Zheng M, Takeda S, Wu M, Peltz G. Humanized thymidine kinase-NOG mice can be used to identify drugs that cause animal-specific hepatotoxicity: a case study with furosemide. The Journal of pharmacology and experimental therapeutics. 2015a; 354:73–78. [PubMed: 25962391]

Xu D, Nishimura T, Nishimura S, Zhang H, Zheng M, Guo YY, Masek M, Michie SA, Glenn J, Peltz G. Fialuridine induces acute liver failure in chimeric TK-NOG mice: a model for detecting hepatic drug toxicity prior to human testing. PLoS Med. 2014; 11:e1001628. [PubMed: 24736310]

Xu D, Wu M, Nishimura S, Nishimura T, Michie SA, Zheng M, Yang Z, Yates AJ, Day JS, Hillgren KM, Takeda ST, Guan Y, Guo Y, Peltz G. Chimeric TK-NOG mice: a predictive model for cholestatic human liver toxicity. The Journal of pharmacology and experimental therapeutics. 2015b; 352:274–280. [PubMed: 25424997]

Zhang Y, Huang SZ, Wang S, Zeng YT. Development of an HSV-tk transgenic mouse model for study of liver damage. The FEBS journal. 2005; 272:2207–2215. [PubMed: 15853805]

Highlights

- Targeted gene disruption on complex genetic backgrounds
- Robust engraftment of human hepatocytes in novel xenorecipient strain
- Persistent HBV viremia in human liver chimeric mice
- Viral suppression upon HBV treatment
- Potential utility for anti-HBV drug testing

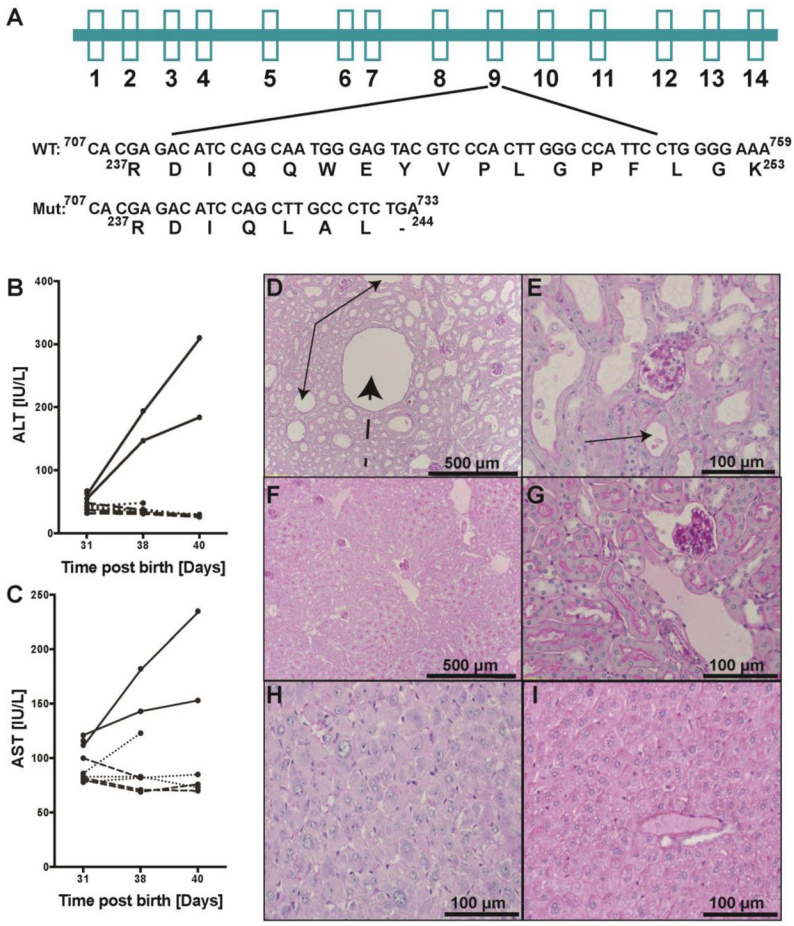

Figure 1. Creation of FAH knockout using ZFN's NOD Rag1−/− IL2Rγ^{NULL} background and characterization of resultant pathology upon NTBC withdrawal

A) Schematic of FAH gene and comparison of exon 9 nucleotide and amino acids sequence between WT and mutant founder #1207 (JR018454). B). Comparison of ALT levels upon withdrawal of NTBC between FAH$^{-/-}$ (solid black line), FAH$^{+/-}$ (thin dotted line), and WT (thick dotted line). C). Comparison of AST levels upon withdrawal of NTBC between WT FAH$^{-/-}$ (solid black line), FAH$^{+/-}$ (thin dotted line), and WT (thick dotted line). D). 100X magnification H&E staining FAH$^{-/-}$ kidney. E). 400X magnification H&E staining FAH$^{-/-}$ kidney. F). 100X magnification H&E staining WT kidney. G). 400X magnification H&E staining WT kidney. H). 400X magnification H&E staining of FAH$^{-/-}$ liver. I). 400X magnification H&E staining of WT liver.

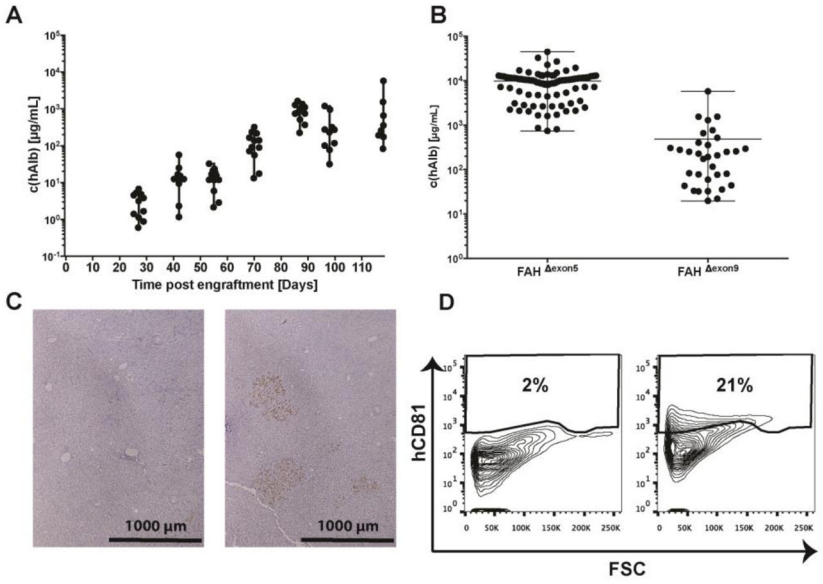

Figure 2. FAH$^{\Delta exon9}$ NRG mice can be robustly engrafted with human hepatocytes

A) Engraftment kinetics of human liver chimeric FAH$^{\Delta exon9}$ NRG mice generated with improved engraftment procedure. B) Comparison between peak hAlb levels in serum of FAH$^{\Delta exon9}$ NRG and FAH$^{\Delta exon5}$ NRG mice. C) Human FAH staining of a FAH$^{\Delta exon9}$ NRG mouse engrafted with human hepatocytes. D). hCD81+ staining and quantification of percent engrafted by flow cytometry of isolated hepatocytes from a FAH$^{\Delta exon9}$ NRG mouse with high engraftment levels as assessed by hAlb ELISA.

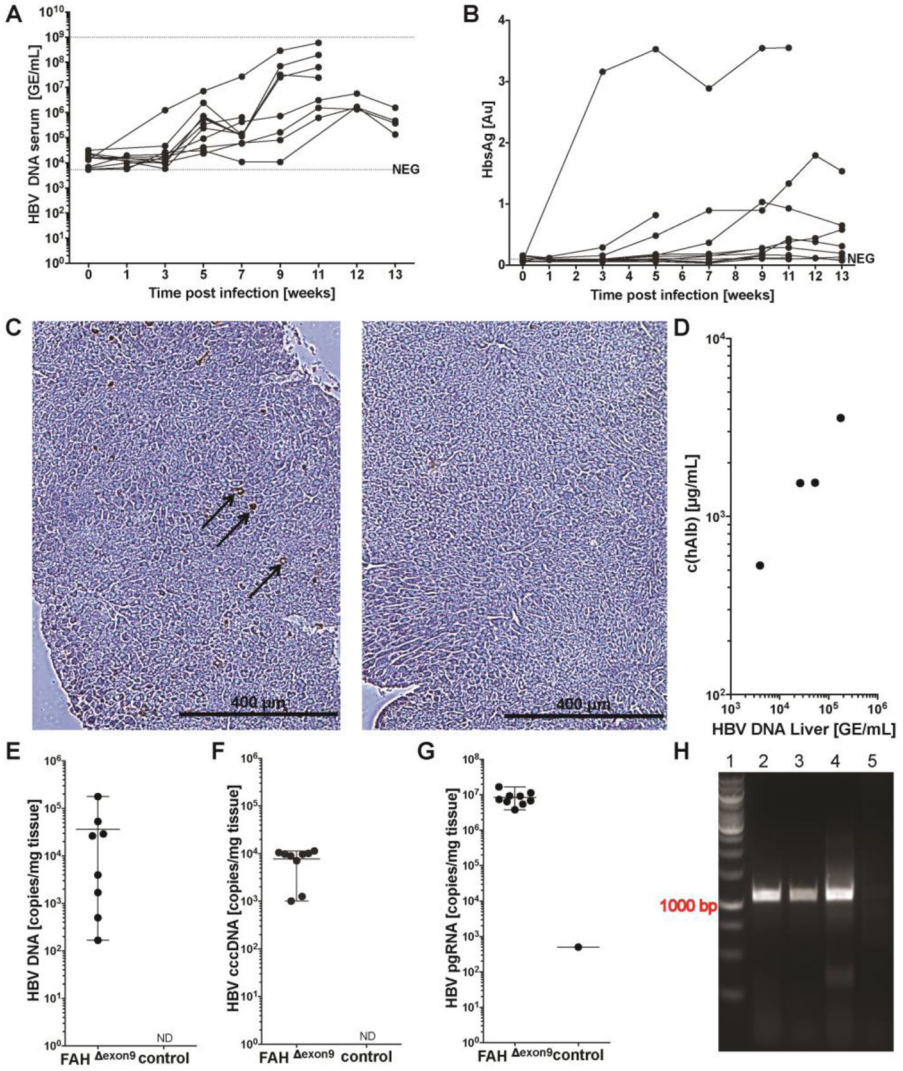

Figure 3. Characterization of HBV infection in FAH$^{\Delta exon9}$ NRG mice

A). Quantification of HBV DNA in serum of HBV challenged mice by qPCR. B). HbsAg ELISA kinetics data. C). HbcAg immunohistochemistry staining of liver sections of a FAH$^{\Delta exon9}$ NRG mouse chronically infected with HBV (right) and uninfected control (left). D). Correlative graph between HBV DNA copies (GE/mg tissue) and hAlb levels show a significant correlation, with higher levels of HBV DNA observed in mice with higher levels of hAlb, i.e. higher engraftment levels. E). Quantification of total HBV DNA in the liver of persistently infected FAH$^{\Delta exon9}$ NRG mice by qPCR. F). Quantification of HBV cccDNA in the liver of persistently infected FAH$^{\Delta exon9}$ NRG mice by qPCR. G). Quantification of HBV pgRNA in the liver of infected mice by RT-qPCR. H). PCR products generated from HBV cccDNA biased primers. Sample templates were of DNA isolated from the liver of infected mice treated with plasmid-safe DNase (lanes 2–4), negative control (lane 5). Lane 1 is molecular weight size marker (1 kb ladder).

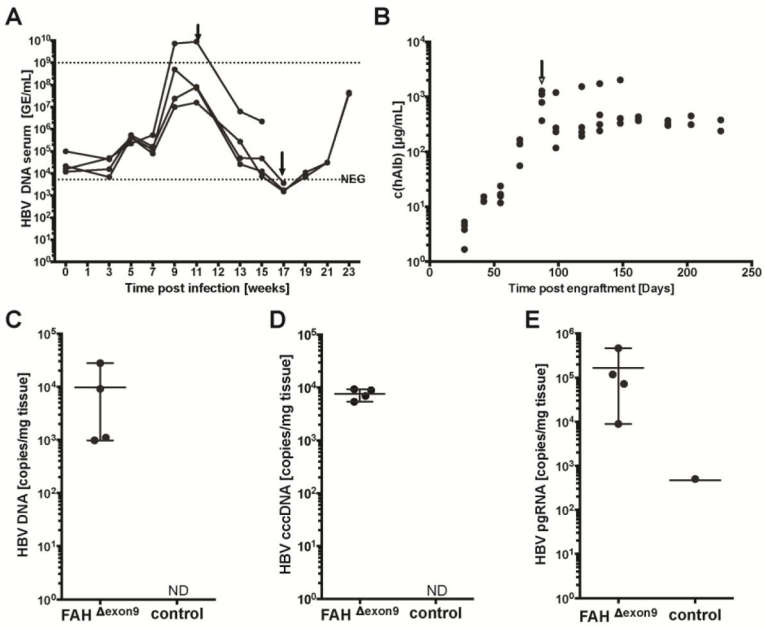

Figure 4. Kinetics of viral parameters of ETV treatment for HBV infected FAH$^{\Delta exon9}$ NRG mice

A). Quantitation of HBV DNA in serum by qPCR. Black arrows indicate start and cessation of ETV treatment. B). hAlb ELISA data confirming mice are stably engrafted with human hepatocytes. Quantification of HBV viral DNA and RNA intermediates determined by qPCR and RT-qPCR respectively C). Total HBV DNA in liver. D). HBV cccDNA in liver. E). HBV pgRNA. The arrow indicates time point when mice were challenged with HBV.